Hindawi Publishing Corporation
International Journal of Photoenergy
Volume 2008, Article ID 482373, 12 pages
doi:10.1155/2008/482373

*Research Article*

# Characterization and Evaluation of the Efficiency of $TiO_2$/Zinc Phthalocyanine Nanocomposites as Photocatalysts for Wastewater Treatment Using Solar Irradiation

**Antonio E. H. Machado,[1] Marcela D. França,[1] Valdemir Velani,[2] Gabriel A. Magnino,[1] Hosana M. M. Velani,[2] Flávio S. Freitas,[1] Paulo S. Müller Jr.,[2] Christian Sattler,[3] and Martin Schmücker[4]**

[1] *Laboratório de Fotoquímica, Instituto de Química, Universidade Federal de Uberlândia, P.O. Box 593, 38400-902 Uberlândia, MG, Brazil*
[2] *Nanobrax, Soluções Tecnológicas e Prestação de Serviços Ltda., Avenida João Naves de Ávila 2121, Bloco 5L, Sala 05, 38408-100 Uberlândia, MG, Brazil*
[3] *German Aerospace Center, Institute of Technical Thermodynamics, Solar Research, Linder Höhe, 51147 Köln Porz, Germany*
[4] *German Aerospace Center, Institute of Materials Research, Linder Höhe, 51147 Köln Porz, Germany*

Correspondence should be addressed to Antonio E. H. Machado, aeduardo@ufu.br

Received 28 August 2007; Revised 23 January 2008; Accepted 17 March 2008

Recommended by Leonardo Palmisano

This work reports the characterization of composites prepared by the association between zinc phthalocyanine (ZnPc) and titanium dioxide. These composites are better photocatalysts for wastewater decontamination mediated by solar radiation than pure $TiO_2$, performance that remains even when reused. The UV-Vis diffuse reflectance absorption spectra show for these composites two intense absorption bands. The first covers the ultraviolet and part of the visible spectrum region until 460 nm (2.7 eV), whereas the second, nonstructured, goes from 475 nm until the near infrared with an absorption peak at 683 nm attributed to the Q band of ZnPc. The production of additional $e^-/h^+$ pairs by these aggregates when photoexcited, their capability to act as charge carrier, the thickness and regularity of their distribution on the $TiO_2$ surface seem to be important parameters for the performance observed for these composites.



## 1. INTRODUCTION

Water recycling by destruction of the pollutant load using advanced oxidative processes (AOPs) has been suggested as an alternative for environmental remediation [1–10]. Between the AOP, heterogeneous photocatalysis can be considered as one of the new "advanced oxidation technologies" (AOTs) for air and water purification [5–7].

For many reasons, $TiO_2$ has been considered as the best choice among the semiconductor oxides with photocatalytic activity for wastewater treatment, aiming the elimination of organic and inorganic species [2, 3, 5–10]. However, its band-gap energy, between 3.0 and 3.2 eV [2, 3], limits its application when solar photocatalysis is desirable [3, 8, 11, 12]. To get round this problem, many research groups have proposed alternatives to amplify the photocatalytic activity of $TiO_2$, improving the pickup of ultraviolet radiation and also making feasible the use of components of the visible radiation [8–20].

Electron transfer at the interface between a photoactive species and the semiconductor surface is a fundamental aspect for organic semiconductor devices [21, 22]. Certain photoactive compounds have proven to be able, when electronically excited, to inject electrons in the conduction band of semiconductors [21–33], increasing the performance of dye-sensitized solar cells. In particular, ultrafast charge separation led by electron injection from electronically excited photoactive molecules to a conduction band of a wide-gap metal oxide, and a good electronic coupling between dye molecules and surface of the substrate are key steps for improving the performance of these materials [23–25].

In this work, we report the characterization by different methodologies, such as diffuse reflectance absorption spectra, specific surface area, thickness of ZnPc coating, and their distribution on the $TiO_2$ particles, evaluated by transmission electron microscopy (TEM) coupled to energy disperse X-ray (EDX) of composites prepared by the association between zinc phthalocyanine (ZnPc) and titanium dioxide. Additionally, the quantum yield of hydroxyl radical production, the capacity of the studied composites to perform the degradation of organic matter present in wastewaters in reactions mediated by solar irradiation, and the possibility of reuse of such photocatalysts were also estimated.

## 2. EXPERIMENTAL

### 2.1. Chemicals

Titanium dioxide, P25, was nicely provided by Degussa Hülls. Zinc phthalocyanine (ZnPc), 98%, acetylacetone, 99%, and a sodium salt of lignossulphonic acid ((LSA), possessing a mean molecular mass of 52,000 D), were purchased from Sigma - Aldrich (São Paulo, Brasil). Methanol, UV/HPLC, dimethylformamide and dimethylsulfoxide, P.A., and ethanol, 95%, were purchased from Vetec Química Fina (Rio de Janeiro, Brasil). Ammonium phosphate buffer (pH 6.0) was prepared using a standard procedure. Potassium ferrioxalate solutions ($10^{-2}$ mol $L^{-1}$) were used as chemical actinometer [34]. All chemicals were used as received.

### 2.2. Preparation of ZnPc/$TiO_2$ composites

The composites were prepared coating $TiO_2$ particles with zinc phthalocyanine [8, 13, 14], dissolved in a solvent mixture containing 50% dimethylsulphoxide, 20% ethanol, and 30% dimethylformamide, at 60°C. The necessary amount of $TiO_2$ (P25, Degussa), covering the compositions of 1.0%, 1.6%, 2.5%, 5.0%, 7.5%, and 10%, was gradually added to the dye solution, under stirring and heating, resulting in a suspension with homogeneous appearance. The suspension was maintained, stirred, and heated until almost complete solvent evaporation. The material, presenting a creamy consistency, was washed several times with distilled water, under vigorous stirring, to remove residues and remaining organic solvent. Next, the composite is dryed at a temperature between 70 and 80°C, for 24 hours. After milling, the final product is a finely divided bluish powder with improved photocatalytic activity [8–14], insoluble in water, capable to give stable suspensions in this solvent.

### 2.3. Characterization

The diffuse reflectance absorption spectra of the composites were recorded using a Shimadzu UV-2501PC spectrophotometer equipped with an integrating sphere. Barium sulphate was used as reference in these experiments.

The specific surface area of the composites was estimated from BET (Brunauer, Emmett, and Teller) isotherms, based on the adsorption of gaseous nitrogen, using a MICROMERITICS ASAP 2000 system.

The thickness of ZnPc coating and their distribution on the $TiO_2$ surface was evaluated by transmission electron microscopy (TEM) coupled to energy disperse X-ray (EDX). TEM investigations were carried out using a Philips Tecnai F30 microscope equipped with a field emission gun, a scanning transmission electron microscope (STEM) and an EDX analytical system. The specimens for TEM analysis were prepared by crushing the powder aggregates in an agate mortar, dispersing in distilled water and depositing onto a carbon film supported by a 300 mesh copper grid.

All measurements were done with unused catalyst.

### 2.4. Quantum yield of hydroxyl radical production ($\Phi_{HO\bullet}$)

The quantum yield of hydroxyl radicals production was estimated using a procedure proposed by Gao et al. [35], based on Nash's method [36]. It consists in the quantification of the formaldehyde concentration formed during the oxidation of methanol by the hydroxyl radicals [37], generated during the photocatalytic process. An aqueous suspension (5 mL), 0.2 mol $L^{-1}$ in methanol, containing $TiO_2$ or one of the composites (50 mg $L^{-1}$), placed in a closed borosilicate glass reactor with a cooling jacket, in which water was continuous circulated to minimize heating by IR irradiation, was photolysed during 30 minutes using a 400 W high-pressure mercury vapor lamp (HPL-N) positioned at 10 cm from the reactor. The suspension was mixed during 20 minutes (magnetic stirrer), prior to illumination and during it.

The radiation was filtered by the borosilicate glass (2 mm thick, cutting below 300 nm), to guarantee the excitation of the catalysts under equivalent conditions. Due to technical limitations, only the light intensity in the UV-A region was monitored during the irradiation. This was done using a solar light PMA-2100 radiometer. The illuminated area was 3.0 $cm^2$.

Formaldehyde formed due to the oxidation of methanol was determined by the Nash method [36], which is based on the Hantzsch reaction: an 1.5 mL aliquot of the photolysed sample, previously filtered using a PTFE Millipore filter (0.45 $\mu$m of porosity), was added to 1.5 mL of 0.18 mol $L^{-1}$ ammonium phosphate buffer (pH = 6.0) and 15 $\mu$L of acetylacetone. A yellow color gradually develops owing to the synthesis of diacetyldihydrolutidine [36]. Under optimum conditions, the molecular extinction in terms of formaldehyde has a smooth maximum of 8,000 $M^{-1}cm^{-1}$ at 412 nm, regardless of dilution. The needed spectrophotometric measurements were done in a range covering this wavelength.

The photonic flux [34] of the mercury lamp was evaluated in the range between 295 and 815 nm using a radiometric/photometric setup built with components furnished by Ocean Optics, Inc. (an SD2000 UV/VIS diode array spectrometer coupled to a personal computer, a fiber optic irradiance probe with a detection head of 0.3 cm diameter, possessing a cosine corrector). These measurements were done using an integration time of 50 milliseconds. A 1 mW He-Ne laser (632.8 nm), two semiconductor lasers (650 and

Figure 1: Details of the CPC reactor experimental setup.

670 nm), and calibrated LEDs (380, 450, 470, and 640 nm of peak output) were used as standards for the quantification of the number of emitted photons. The radiation that can be effectively absorbed by these catalysts was considered as being in the 295 to 710 nm range, with a photonic flux of about of $3.3 \times 10^{-6}$ einsteins $s^{-1}$.

### 2.5. Photodegradation essays

The capacity of the studied composites to degradate organic matter present in wastewaters, in reactions mediated by solar irradiation, and the possibility of reusing of such photocatalysts was evaluated monitoring the decrease of the organic matter content during the treatment of three 50 L batches of a model effluent (an aqueous solutions containing 160 mg $L^{-1}$ of LSA) [8]. The reactions were done at pH 3, with the addition of 1 mL of $H_2O_2$ 30% v/v per liter of effluent (about 9 mM), and monitored by chemical oxygen demand (COD) analysis of aliquots of effluent samples collected at different accumulated doses of UV-A radiation. (This option was due to operational limitations. The spectral pattern of the visible light does not change significantly during the execution of the experiments.) To evaluate the observed (global) reaction kinetics, the temporal variations were substituted by the UV-A accumulated dose, which warrants the reproduction of these experiments under different latitude and weather conditions.

A same sample (100 mg per liter of effluent) of the photocatalyst, containing initially 2.5% of ZnPc, was used to treat the three effluent batches. The treatment of each batch was performed using a compound parabolic concentrator (CPC) reactor, after the recovery of the photocatalyst used in the previous experiment.The CPC reactor was constructed in our laboratory [11, 12]. It was designed to process up to 150 L of effluent. This reactor consists in a module with an aperture of about 1.62 $m^2$, elevation angle adjusted to the latitude of Uberlândia, Brasil (19°S), containing 10 borosilicate glass tubes (external diameter 32 mm, wall thickness of 1.4 mm, and length of 1500 mm), mounted in parallel, each on double parabolic-shaped aluminum reflector surfaces (Figure 1). The concentration ratio is about 1.0 and the reflectivity of the reflector surface within the band gap of $TiO_2$ (300–390 nm) is 89.5%. The flow rate is 34 L $min^{-1}$. The effluent was circulated in the reactor which is open to guarantee a sufficient oxygen concentration in the bulk. The fluid flow rate in the tubing was chosen to assure a turbulent transport regimen of the effluent, warranting a better homogenization of the suspension. This and the fact that the irradiated effluent returns to the reservoir by a tubing positioned 50 cm above the surface of the remaining effluent guarantees an adequate aeration of the effluent during the photocatalytic process. The fittings and piping were made of polypropylene.

This reactor is similar to the SOLARDETOX prototypes used at the Plataforma Solar de Almería and the German Aerospace Center, Cologne [38, 39], but the mirrors were calculated exclusively for this reactor and the ratio between irradiated surface and dark tubing is higher. Since the BRITE EURAM SOLARDETOX project CPC-type reactors are known as very powerful solar reactors for water treatment up to a pilot plant scale [38, 39].

As reference, an additional effluent batch was treated under similar conditions using pure $TiO_2$ P25 as catalyst.

For all reactions, hydrogen peroxide (30 mg $L^{-1}$) was used as additional source of reactive species [8].The incident UV-A radiation was monitored using a solar light PMA-2100 radiometer. All reactions were stopped when the accumulated dose of UV-A radiation reached 900 kJ $m^{-2}$.

The COD measurements were based on an Environmental Protection Agencies recommended method [40, 41], in which an aliquot of the effluent reacts under heating and closed reflux, at 423 K during 2 hours, reducing dichromate ions to chromic ions in a strongly acid medium. From absorbance measurement, done at 620 nm using a Hach DR-4000U spectrophotometer and a resident program, the COD of the samples was determined.

## 3. RESULTS AND DISCUSSION

### 3.1. Diffuse reflectance spectra

Figure 2 presents the diffuse reflectance spectra of ZnPc, $TiO_2$, and some of the studied composites.

Comparison of these figures shows that the UV-Vis absorption spectrum of these composites is not simply the result of an additive effect between the absorption spectra of $TiO_2$ and zinc phthalocyanine (ZnPc) (compare Figures 2(a), 2(e), and 2(f)). The later figure corresponds to the diffuse reflectance spectra of pure ZnPc. The intense absorption peak at 552 nm, is due to the Q band, relative to $\pi \rightarrow \pi^*$ transitions [42, 43]. The observed blue shift for this peak can be attributed to noninteracting molecules and the absence of interaction between them and solvents [42, 44]. The Soret band is evident in the ultraviolet, with an absorption maximum at 301 nm. A low intensity and nonstructured absorption band with the absorption peak centered at 416 nm is related to an $n \rightarrow \pi^*$ transition linking the $e_u$ azanitrogen lone pair orbital with the $e_g$ LUMO [43, 45]. A set of three very small low-energy bands, above the Q one, can also be observed. The spectral structure of ZnPc and $TiO_2$ is lost in the composites. For the spectrum of the composite with 2.5% m/m of ZnPc obtained using pure $TiO_2$ as a reference, for example, the bands in the ultraviolet and visible are very different from that observed for pure ZnPc. In the visible, presents a large and intense three peak band

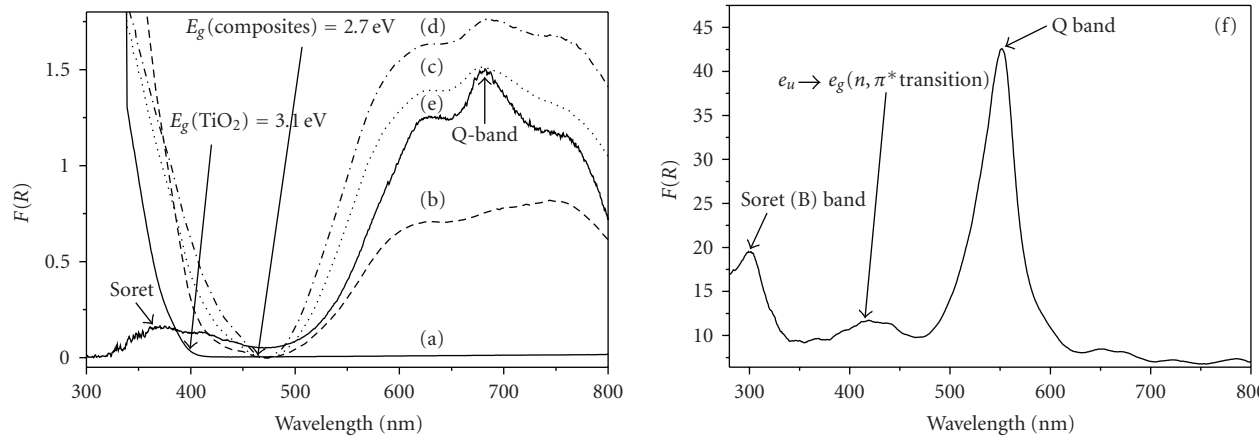


FIGURE 2: Diffuse reflectance spectra of $TiO_2$/ZnPc composites, prepared with different percent in mass of ZnPc: (a) $TiO_2$ P25. Composite containing: 1.0% of ZnPc (b); 2.5% of ZnPc (c); 5.0% of ZnPc (d); (e) composite containing 2.5% of ZnPc ($TiO_2$ P25 was used as reference), showing the Soret (370 nm) and Q (683 nm) bands, typical of ZnPc; (f) diffuse reflectance spectrum of pure ZnPc. Barium sulphate was used as reference for (a) to (d).

centered by a red-shifted Q band, with maximum at 683 nm [12]. The Soret (B) band presents a different shape and is red shifted when compared to its equivalent in Figure 2(f).

Thus, these absorption spectra are very different from the typical absorption profiles of $TiO_2$ (Figure 2(a)) and pure ZnPc in the solid state (Figure 2(f)) and in very dilute liquid solutions [44]. The absorption spectrum of these composites is characterized by an intense absorption band below 460 nm, and a large and intense absorption band, above 475 nm, most probably due to an extense superposition of the electronic states of $TiO_2$ and ZnPc, indicating electronic interaction between both species, resulting in several common electronic states for both species. Szaciłowski et al. [46] reported in a recent work that the diffuse reflectance spectrum of $TiO_2$/prussian blue does not correspond directly to the sum of the spectra of both components, indicating electronic interaction between the particulate semiconductor and the polymeric matrix.

The spectrum shown in Figure 2(e) is very similar to the absorption spectrum for a flash-evaporated ZnPc thin film deposited on a glass substrate, as reported by Senthilarasu et al. [47], in which the two energy bands characteristic of phthalocyanines is evident, one in the region between 500 and 900 nm, with an absorption peak at 690 nm, related to the Q band, and the other, very intense, at 330 nm, attributed to Soret (B) band [48]. Mi et al. have reported a similar absorption spectrum for thin films of Magnesium Phthalocyanine [49]. The unstructured visible region band and the red shift of the Q band of these composites can be attributed to the strong intermolecular interactions due to ZnPc aggregation ($ZnPc_{agg}$), resulting in exciton coupling effects of the allowed transitions. This causes an important charge carrier mobility, as suggested by Hoffmann [50], or to the lift of degeneracy increasing the band splitting due to molecular distortion [49, 51, 52]. Based on the spectral characteristics of these composites, mainly in the visible, we can conclude that the excitons formed by the aggregation of ZnPc molecules behave as Frenkel's J aggregates [53, 54].

The $E_g$ value for ZnPc/$TiO_2$ composites, estimated by diffuse reflectance, is lower (2.7 eV) than the one observed for pure $TiO_2$ (between 3.0 and 3.2 eV) [2, 3], and similar to the value for iron(II) phthalocyanine excitons (2.6 eV) in FePc/$TiO_2$ blends [55] and other metal phthalocyanine associated to semiconductor oxides [16]. For ZnPc thin films, Senthilarasu et al. [47] have assigned an $E_g$ of 1.97 eV, with a directly allowed optical transition, near to the value estimated by us for the peak absorption Q-band (2.25 eV) of pure ZnPc in the solid state (Figure 2(f)).

The $E_g$ for these composites might be related to the electronic coupling between $TiO_2$ and ZnPc, and its positive implications. Similar to FePc/$TiO_2$ blends [55] and ZnPc thin films [22, 47], the photoexcitation of ZnPc aggregates results in the formation of $e^-$/$ZnPc^+$ pairs, parallel reactions from these species and the electron injection from these ZnPc excitons to bulk $TiO_2$, which explains at least in part the improved photocatalytic activity observed for some of the ZnPc/$TiO_2$ composites [11, 12]. The electronic coupling strength between donor and acceptor is one of the critical factors for electron transfer to occur [22, 23, 47, 48]. Experiments based on femtosecond pump-probe laser spectroscopy have provided valuable information for understanding the electron transfer from excited dye molecules to nanocrystalline $TiO_2$ films or $TiO_2$ nanoparticles [25, 56–58]. Sharma et al. [55] observed a strong photoluminescence quenching of FePc in FePc/$TiO_2$ composite film, while the photosensitivity of a device formed by FePc/$TiO_2$ composite sandwiched between Al and ITO is significantly enhanced when compared to pure FePc film. The authors concluded that both effects arise from the charge transfer from FePc to $TiO_2$ and charge separation after photoexcitation, resulting in FePc($h^+$) and $TiO_2$($e^-$). Additionally, they reported that the charge transport and the current leakage through FePc

films and the photogeneration are due to the efficient dissociation of exciton at the donor-acceptor interface of the bulk, and that the higher holes mobility in the organic material layer, combined with lower conductance leakage, leads to the more efficient collection of photogenerated carriers.

The excited-state dynamics of metal phthalocyanines in solution and thin filmshas been extensively studied by transient absorption spectroscopy and time-resolved photoluminescence measurements [47, 49, 59]. Despite the occurrence of several $S_1$ state relaxation processes in thin solid films (fluorescence, internal conversion, intersystem crossing, ultrafast exciton-exciton annihilation, exciton-phonon coupling), the nonradiative processes tend to be predominant [49, 60, 61]. The fluorescence quantum yields, for example, tend to be extremely low in thin films owing to enhanced intersystem crossing [61]. Sakakibara et al. in studies on photoluminescence properties of phthalocyanine solid films, observed that fluorescence quantum yields at room temperature were reduced to $10^{-5}$–$10^{-4}$, much smaller than those of the corresponding monomers (>0.5) [61]. In addition to these relaxation processes, if these films are deposited onto bulk $TiO_2$, the electron transfer from metal phthalocyanine excitons has been reported [22, 55, 59].

### 3.2. Transmission electron microscopy

For composites containing 1%, 2.5%, and 5% m/m of ZnPc, coatings of ZnPc with irregular thickness covering the $TiO_2$ grains were observed (Figures 3(a)–3(c)). For the first one, the coating thickness varies between 0 and 10 nm, whereas for the composite containing 5% m/m of ZnPc, thicknesses between 0 and 25 nm were observed.

On the other hand, the composite containing 2.5% m/m of ZnPc presented the most regular coating thickness, ranging between 5 and 10 nm. Some uncoated surface areas also occur but to a much lower degree than verified for the other compositions.

ZnPc amounts exceeding about 2.5% lead to an increasingly unhomogeneous distribution. Microstructural investigations and energy dispersive X-ray (EDX) analyses of the 5% m/m coated composite (Figure 4) reveal two different regions: amorphous areas consisting of aggregates rich in carbon, zinc and sodium and crystalline regions formed by almost pure agglomerates of $TiO_2$. Signals corresponding to copper, from TEM support grids, can be also observed. Sodium observed in the amorphous areas was probably incorporated during the preparation of the samples.

### 3.3. Quantum yield of production of hydroxyl radicals

The following set of reactions [3, 17] can be considered an approximate representation of the main reactions involved in the photocatalytic process induced by $TiO_2$ and composites on methanol degradation:

$$TiO_2 \xrightarrow{hv} TiO_2/e^-_{CB} + TiO_2/h^+, \quad (1)$$

$$ZnPc_{agg} \xrightarrow{hv} {}^1(ZnPc_{agg})^*, \quad (2)$$

$${}^1(ZnPc_{agg})^* \xrightarrow{isc} {}^3(ZnPc_{agg})^*, \quad (3)$$

$$(ZnPc_{agg})^* + O_2 \longrightarrow O_2{}^{\bullet -} + (ZnPc_{agg})^+, \quad (4)$$

$$(ZnPc_{agg})^* \longrightarrow e^-_{CB}/ZnPc^+_{agg}, \quad (5)$$

$$e^-_{CB}/ZnPc^+_{agg} + TiO_2 \longrightarrow ZnPc^+_{agg} + TiO_2/e^-_{CB}, \quad (6)$$

$$H_2O + h^+_{VB} \longrightarrow HO^\bullet + H^+, \quad (7)$$

$$H_2O + O_2{}^{\bullet -} \longrightarrow HO_2{}^\bullet + HO^-, \quad (8)$$

$$e^-_{CB} + O_2 \longrightarrow O_2{}^{\bullet -}, \quad (9)$$

$$2O_2{}^{\bullet -} + 2H_2O \longrightarrow H_2O_2 + O_2 + 2HO^-, \quad (10)$$

$$e^-_{CB} + H_2O_2 \longrightarrow HO^\bullet + HO^-, \quad (11)$$

$$HO^\bullet + CH_3OH \longrightarrow {}^\bullet CH_2OH + H_2O, \quad (12)$$

$$HO^\bullet + {}^\bullet CH_2OH \longrightarrow HCHO + H_2O, \quad (13)$$

$${}^\bullet CH_2OH + O_2 \longrightarrow {}^\bullet O_2CH_2OH \longrightarrow HCHO + HO_2{}^\bullet, \quad (14)$$

$$HO^- + h^+_{VB} \longrightarrow HO^\bullet, \quad (15)$$

$$TiO_2/(ZnPc_{agg}) + h^+_{VB} \longrightarrow TiO_2/(ZnPc_{agg})^+, \quad (16)$$

$$TiO_2/(ZnPc_{agg})^+ + HO^- \longrightarrow TiO_2/(ZnPc_{agg}) + HO^\bullet, \quad (17)$$

$$(ZnPc_{agg}) + HO^\bullet \Longrightarrow \text{oxidation products}, \quad (18)$$

$$TiO_2/(ZnPc_{agg})^+ + CH_3OH \Longrightarrow \text{oxidation products}, \quad (19)$$

$$2HO^\bullet \longrightarrow H_2O_2, \quad (20)$$

$$H_2O_2 + O_2{}^{\bullet -} \longrightarrow HO^\bullet + HO^- + O_2, \quad (21)$$

$$H_2O_2 + h^+_{VB} \longrightarrow HO_2{}^\bullet + H^+, \quad (22)$$

$$TiO_2/(ZnPc_{agg})^+ + H_2O_2 \longrightarrow HO_2{}^\bullet + H^+ + TiO_2/ZnPc_{agg}, \quad (23)$$

$$2HO_2{}^\bullet \longrightarrow H_2O_2 + O_2, \quad (24)$$

$$2HO_2{}^\bullet + O_2{}^{\bullet -} \longrightarrow HO^\bullet + HO^- + 2O_2. \quad (25)$$

The methodology used to estimate the quantum yield of hydroxyl radicals production [35–37] can be considered useful and safe since the reactions related to the generation of hydroxyl radicals are sufficiently fast. For example, reaction (12) presents expressive values for the rate constant, in the range between 8.3 and $9.7 \times 10^8$ L mol$^{-1}$ s$^{-1}$ [62, 63], whereas reaction (13), between the dehydro-methanol radical and $HO^\bullet$, the bimolecular rate constant is in the limit for diffusion-controlled reactions ($10^9$–$10^{10}$ L mol$^{-1}$ s$^{-1}$). On the other hand, the trapping of hydroxyl radicals by hydrogen peroxide, a possible side reaction, occurs at a considerably slower rate ($2.7 \times 10^7$ L mol$^{-1}$ s$^{-1}$) [62]. The primary steps that culminate in the formation of $HO^\bullet$ are also in the limit for diffusion-controlled reactions.

Figure 5 shows the expected dependence between the quantum yield of hydroxyl radicals generation ($\Phi_{HO\bullet}$) and the amount of ZnPc adsorbed on $TiO_2$ for experiments at the laboratory scale (Section 2.4). Initially, an increase in the $\Phi_{HO\bullet}$ is observed, with a maximum value ($\Phi_{HO\bullet} = 0.60$)

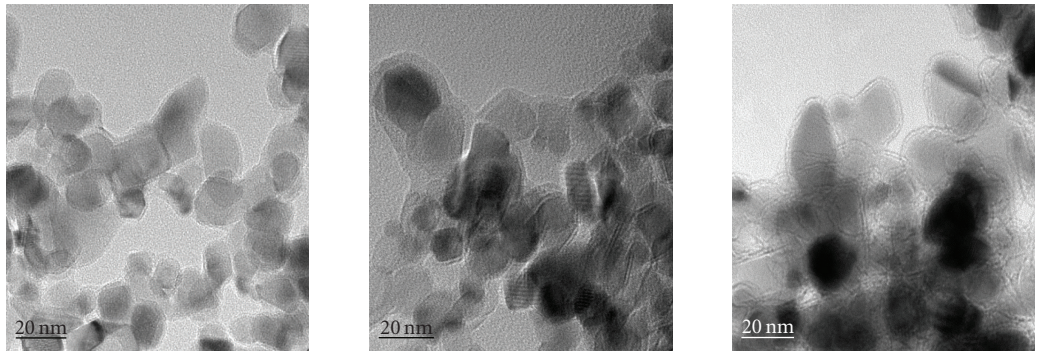


Figure 3: Transmission electron micrographs of granules of the different $TiO_2$/ZnPc composites: (a) 1% ZnPc, (b) 2.5% ZnPc, and (c) 5% ZnPc.

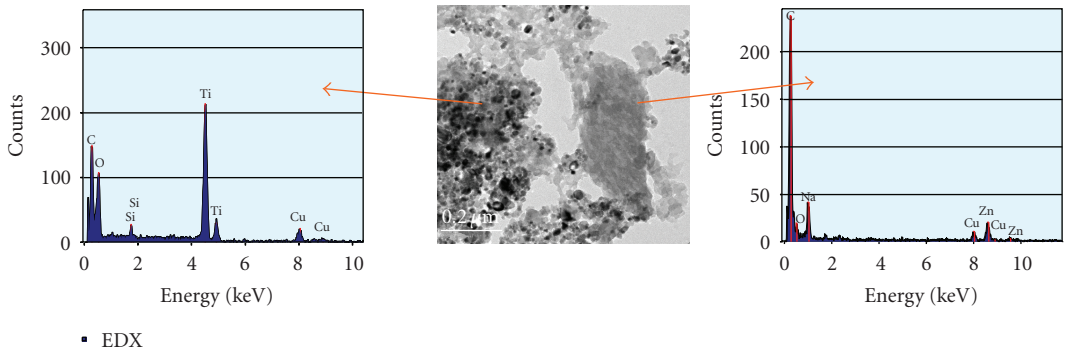


Figure 4: Transmission electron micrography and X-ray dispersive energy of the composite containing 5% of ZnPc.

for a ZnPc concentration equals to 2.5% m/m. For pure $TiO_2$, $\Phi_{HO\bullet}$ is 0.06.A similar trend should be expected during solar photocatalysis. However, since hydrogen peroxide is involved as an additional source of hydroxyl radicals [8–12], it is expected that this must cause a significant increase in $\Phi_{HO\bullet}$. Sun and Bolton [37], investigating the generation of hydroxyl radicals by aqueous suspensions of $TiO_2$ (Anatase, Aldrich), reported $\Phi_{HO\bullet}$ changed from 0.04 to 0.22 with the addition of hydrogen peroxide in the reactional medium. They also observed that when the $H_2O_2$ concentration in the suspension is larger than 18 mM, a plateau for the $\Phi_{HO\bullet}$ values is reached. The presence of $H_2O_2$ in the suspension might influence the redox reactions occurring at the $TiO_2$ particles surface, acting as electron acceptor, competing with the $O_2$, reactions (9) and (11), in the redox reactions, and also producing additional $HO^\bullet$ radicals, reactions (11), (21), (22), and (23). According to the data published by Sun and Bolton [37], the $H_2O_2$ concentration (about 9 mM) used in our experiments under solar irradiation is capable of increasing $\Phi_{HO\bullet}$ at least 4.5 times.

In principle, the light intensity ($1.1 \times 10^{-6}$ einsteins $s^{-1}\,cm^{-2}$) in the 295 to 710 nm range, capable to trigger the photocatalytic processes mediated by the composites in the experiments at the laboratory scale, also could accelerate the $e^-/h^+$ recombination, impairing the production of $HO^\bullet$ radicals, implying in $\Phi_{HO\bullet}$ values lower than desired [35, 37]. However, it is probable that, at this wavelength range, nor all photons are capable to generate $e^-/h^+$ pairs in $TiO_2$, or favor the electron injection from ZnPc excitons to bulk $TiO_2$. An estimate based on the spectral distribution of the mercury lamp shows that the light intensitybetween 295 and 390 nm, capable to photoexcite $TiO_2$, generating $e^-/h^+$ pairs, is about $2.0 \times 10^{-7}$ einsteins $s^{-1}\,cm^{-2}$. The light intensity between 295 and 460 nm, $3.9 \times 10^{-7}$ einsteins $s^{-1}\,cm^{-2}$, should be capable to photoexcite $TiO_2$/ZnPc composites, generating $e^-/h^+$ pairs in both species, and consequently favoring the electron injection from ZnPc excitons to $TiO_2$ conduction band (Scheme 1), since in this wavelength range the superposition of the electronic states of $TiO_2$ and ZnPc implies in several common electronic states for both species. The rest of the emitted photons,between 460 and 710 nm (about $5.1 \times 10^{-7}$ einsteins $s^{-1}\,cm^{-2}$), should be related to other processes directly mediated by the ZnPc excitons formed by the electronic excitation in this wavelength range. This explains the reason by which the estimated $\Phi_{HO\bullet}$ value in our measurements using pure $TiO_2$ (Degussa P25) is equal to 0.06, 50% higher than the value estimated by Sun and Bolton [37] for aqueous suspensions of pure $TiO_2$ (anatase), but equivalent to the value reported for $TiO_2$ Degussa P25 ($\Phi_{HO\bullet} \approx 0.06$) [64]. Several authors have shown that $\Phi_{HO\bullet}$ is inversely proportional to the square root of the incident light intensity [35, 37, 65, 66], behavior attributed to an

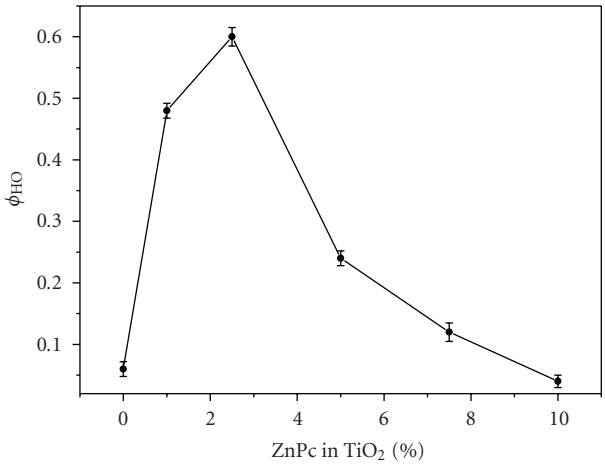


Figure 5: Dependence between the hydroxyl radicals quantum yield and the amount of zinc phthalocyanine adsorbed on $TiO_2$.

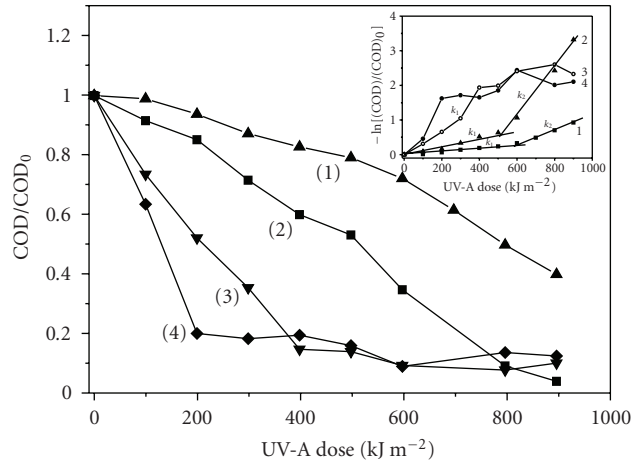


Figure 6: Degradation of the organic load present in 50 L of an aqueous model-effluent containing LSA (160 mg/L). Reactions done proceeded at pH 3, using 100 mg of catalyst per liter of effluent, and addition of 1.00 mL of hydrogen peroxide per liter of effluent. Effluent treated using: (1) pure $TiO_2$; (2) $TiO_2$/ZnPc 2.5% composite; (3) a recycled $TiO_2$/ZnPc 2.5% composite; (4) $TiO_2$/ZnPc 2.5% in its second recycle. *Inset*: Pseudofirst-order rate profiles for the effluent degradation under the above mentioned conditions.

increase in the production rate of $e^-/h^+$ pairs, which favors the electron/hole recombination, thus decreasing the relative number of photoinduced carriers taking part in the redox reactions at the catalyst surface [35, 37]. On the other hand, as occurs in the solar photocatalytic process [8–12], the addition of $H_2O_2$ should contribute to reducing the recombination of photoinduced electrons and holes [37], which must increase the $\Phi_{HO\bullet}$.

Based on these facts, considering the $TiO_2$/ZnPc composites, the participation of excitons formed by electronic excitation of the ZnPc aggregates is not only restricted to the electron injection into the conduction band of $TiO_2$, which must occur only at wavelengths lower than 460 nm. Other processes should be triggered by these charge carriers, especially after electronic excitation at wavelengths higher than 460 nm, otherwise, we should observe a strong quenching of the photocatalytic activity and not a synergic behavior involving $TiO_2$ and $ZnPc_{agg}$ (observed in results to be published). This synergism explains the higher $\Phi_{HO\bullet}$ values estimated for three of the studied composites (Figure 5).

Although the values estimated by us $\Phi_{HO\bullet}$ are not definite, they suggest an important trend, since they converge to the results obtained in studies involving the photocatalytic degradation of organic matter, mediated by solar radiation, that show some $TiO_2$/ZnPc combinations present significant increments in their photocatalytic activity. For example, the ratio between $\Phi_{HO\bullet}$ for the composite containing 2.5% m/m of ZnPc and the estimated for pure $TiO_2$ shows an improvement of at least 1000% in the production of hydroxyl radicals.

The comparison of the photocatalytic degradation of the organic matter (LSA) present in a model effluent [8–10], promoted by these composites and pure $TiO_2$ in a solar photocatalytic process, confirms the better performance of the first ones, especially the composite containing 2.5% m/m of ZnPc, to perform wastewater treatment using photocatalytic processes mediated by solar irradiation [11, 12].

Despite the fact that part of the adsorbed ZnPc is degraded during the photocatalytic process, surprisingly, the photocatalytic efficiency of the recovered composite does not decrease significantly when reused. Preliminary results (not shown) suggest that a load of composite can be used at least five times before presenting photocatalytic efficiency similar to pure $TiO_2$. This can be due to, in great part, the gradual ZnPc degradation, which occurs during the cycles of use of the catalyst. In a minor extent, limited by its very low water solubility, ZnPc also tends to migrate to the aqueous medium.

Figure 6 shows an increase in the degradation rate, with significant changes in the degradation profile due to the use of a recovered composite. This suggests that some reactions, less probable to occur in virtue of ZnPc aggregates formation, become important for the global process. For example, the production of singlet oxygen from $^3$ZnPc* can be a plausible event if the level of ZnPc aggregation is drastically lowered, which is consistent with the fact that photoactive compounds like ZnPc, when aggregated, are incapable to sensitize type I and II reactions [67, 68]. This behavior is attributed to the fact that aggregates in the electronically excited state tend to be deactivated preferentially by nonradiative processes [68]. On the other hand, the better hydration of the catalyst surface, due to many cycles of use, should favor reactions involving the holes (Scheme 1).

For ZnPc concentrations above 2.5%, $\Phi_{HO\bullet}$ tends to decrease, most probably due to the occurrence of undesirable processes related to the increasing size of the ZnPc aggregates, such as exciton-exciton annihilation due to the excessive coating of the $TiO_2$ surface. Essays involving a ZnPc/$SiO_2$ composite coated with 2.5% m/m of ZnPc reinforce, as expected, that the observed process is not

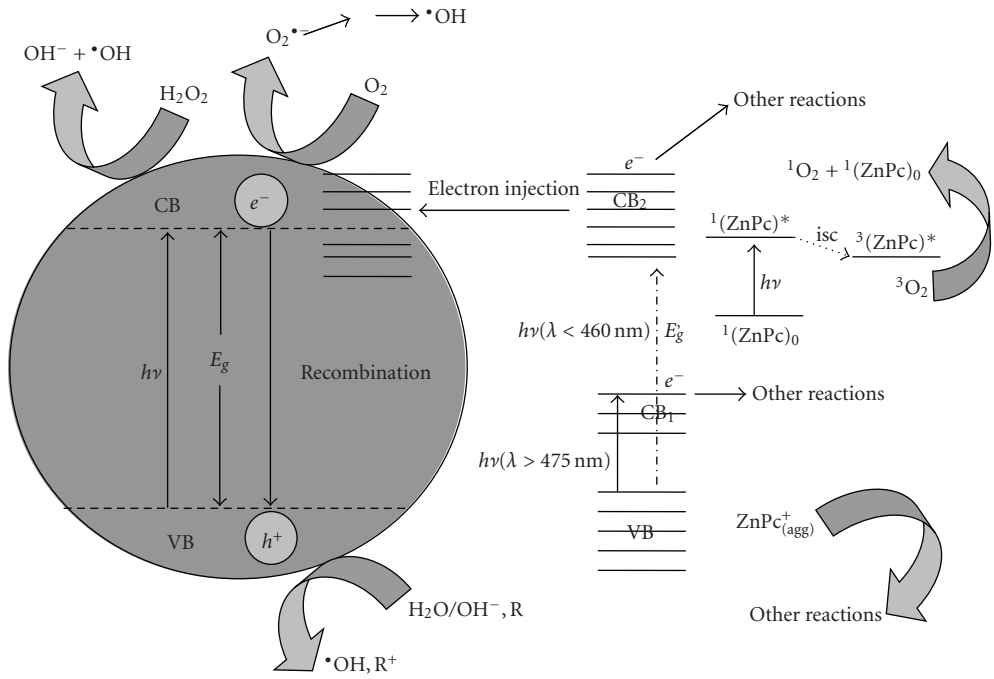


Scheme 1: Main processes involved in a photocatalytic process mediated by a $TiO_2$/ZnPc composites.

exclusively due to ZnPc or $TiO_2$, but to a synergism between these species, indeed when the composite is excited by visible radiation (unpublished results).

It is well known that the degradation of organic matter induced by photocatalysis follows Langmuir-Hinschelwood kinetics [3, 8]. Assuming the concentration of reactive species quickly reaches a stationary state at the beginning of the photocatalytic process [8], the global rate law seems to follow pseudofirst-order behavior with respect to the organic matter (Figure 6-Inset).

The adsorption of the organic matter at the surface of the catalyst in this situation occurs at a low rate [8], since that LSA is constituted by fragments of large size and molecular mass. The formation and desorption of reactive species, derived from small molecules (water, $H_2O_2$, $O_2$, undegraded small fragments of LSA, etc.) should compensate the slow adsorption rate of the large fragments, reacting with them in the catalyst/solvent interface. Considering this aspect, we can consider that LSA degradation is a particular case in which at least one of the steps does not follow the Langmuir-Hinshelwood mechanism.

In the experiments using solar irradiation, to permit comparison with the results obtained under different latitude and weather conditions, it is necessary to use UV-A accumulated dose instead of the temporal variation data. Therefore, the estimated parameters refer to a constant related to the COD decrease rate relative to the variation of the accumulated dose of UV-A radiation. These constants were calculated considering an expression similar to the first-order reaction rate law in which the term $d(\mathrm{COD})/dt$ was substituted by $d(\mathrm{COD})/d(\mathrm{dose})$, since $d(\mathrm{dose}) \propto dt$. As COD is dimensionally equivalent to the concentration of organic matter, the calculated constant (now named *degradation constant*, $D$) has the dimensions of the reciprocal of the radiation dose. The monitoring of only the UV-A dose was adopted exclusively due to operational limitations. However, this should have only a minor effect on the results since the spectral pattern of the visible light between a set of experiments does not vary significantly.

The *degradation constants*, $D$, calculated for the degradation of LSA mediated by $TiO_2$ and $TiO_2$/ZnPc 2.5% are presented in Table 1. Using pure $TiO_2$ or an unused sample of the composite as catalyst, the reaction seems to occur in two steps being the second faster than the first one. The observed increase in the *degradation constant* of the second step is most probably due to the increasing hydration of the surface of the catalyst and the participation of new reactive species. These results also confirm previous results which show that the apparent rate constant for reactions mediated by these composites are systematically higher than the ones using pure $TiO_2$ [8, 11, 12].

The *degradation constant* for the first step of the reaction mediated by the composite containing 2.5% m/m of ZnPc, ($D_1$), is about 130% higher than the one for pure $TiO_2$, whereas the corresponding value for the second step is 3,300% higher. Although premature to present conclusions on the involved processes, a comparison between these values and the estimated increase in $\Phi_{HO\bullet}$ reinforces that the photocatalytic processes triggered by these composites is much more complex than the process catalyzed by pure $TiO_2$ [3], as suggests the set of reactions presented in Section 3.3.

The two steps trend is also verified in the degradation mediated by reused composite. However, in this case $D_2$ seems do be near zero. The estimated value for the

Table 1: Degradation constants ($D$) for LSA degradation under different conditions.

| Catalyst | $D_1$ ($m^2J^{-1}$) | $D_2$ ($m^2J^{-1}$) | $D_1$ ($X$)/$D_1$ ($A$) | $D_2$ ($X$)/$D_2$ ($A$) |
|---|---|---|---|---|
| Pure $TiO_2$ ($A$) | $5.6 \times 10^{-7}$ | $2.0 \times 10^{-6}$ | 1.0 | 1.0 |
| $TiO_2$/ZnPc 2.5% ($B$) | $1.3 \times 10^{-6}$ | $6.7 \times 10^{-6}$ | 2.3 | 34 |
| Composite after reuse ($C$) | $4.2 \times 10^{-6}$ | — | 7.5 | — |

$X = A$, $B$, or $C$.

Table 2: Specific surface area values for $TiO_2$ and $TiO_2$/ZnPc composites at different m/m ratios.

| Composition | SSA ($m^2g^{-1}$) |
|---|---|
| P25 | 52 |
| $TiO_2$/FtZn 1% | 38 |
| $TiO_2$/FtZn 2.5% | 35 |
| $TiO_2$/FtZn 5% | 36 |

*degradation constant* of the first step ($D_1$) of these processes is valid until an accumulated UV-A dose of about 600 kJ $m^{-2}$ (Figure 6-Inset) and is 650% higher than the observed value for the first step of the process mediated by pure $TiO_2$, and 230% higher when compared with the first one for the composite used for the first time.

As a consequence of the reactions triggered by the composite containing 2.5% m/m of ZnPc after the first time use,the final COD of the effluent after an accumulated UV-A dose of 900 kJ $m^{-2}$ (this value corresponds to about 3 hours of solar irradiation during a sunny day, or 5 to 6 hours during a day with moderate to high nebulosity, in Uberlândia, MG, Brasil [12]) corresponds to 4% of the initial value. For a reused composite, this value corresponds to 9%, whereas using pure $TiO_2$ under similar conditions, the observed reduction in COD was of 60%.

Although it is possible to perform the photocatalytic treatment until complete mineralization of the organic matter, often it is economically more suitable to use the photocatalytic process as an effluent pretreatment, completing the treatment with othermore efficient processes. In a previous investigation [10], a treated lignosulphonate wastewater was tested for its biochemical oxygen demand (BOD). The results observed suggest that when a high bioavailability is reached at the point where the performance of the photocatalytic treatment decreases, its discontinuation and the beginning of a treatment based on the biological degradation technology is more favorable.

### 3.4. Specific surface area

Table 2 shows the specific surface area (SSA) of pure $TiO_2$ and of ZnPc-coated $TiO_2$, at different concentrations.

The SSA of the composites is about 30% smaller than the one of pure $TiO_2$, suggesting ZnPc adsorption reduces the $TiO_2$ porosity. The changes in the SSA of the composites do not imply in distortions of the $TiO_2$ crystal structure. For pure $TiO_2$ and composites, the peak positions and lattice parameters of the anatase and rutile phases (not shown) remain practically unchanged, supporting the structural integrity of the $TiO_2$ phases. The increase in the amount of dye results in a decrease of the relative intensity of the peaks, evidencing the adsorption of the dye on the semiconductor surface, and a partial absorption of the incident radiation by the dye.

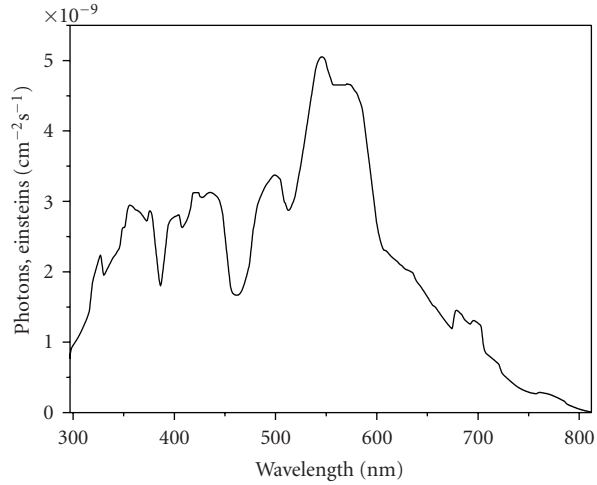


Figure 7: Spectral distribution of the radiation emitted by a 400 W HPL-N mercury lamp in the 295 to 815 nm spectral range.

X-ray powder diffraction patterns of $TiO_2$ and the different composites only show peaks due to the anatase and rutile phases (figure not shown), suggesting ZnPc is adsorbed on the semiconductor surface. This agrees with the results based on scanning tunneling microscopy using different metal phthalocyanines, which concluded that this class of compounds lies flat on the semiconductor surface [69].

### 3.5. Final remarks

The spectral distribution of a 400 W high-pressure (HP) mercury lamp, in the 295 to 815 nm range, is shown in Figure 7 .

The analysis of the spectral distribution shows that the photonic flux in the 295 to 390 nm range, useful for the electronic excitation of pure $TiO_2$, ZnPc, and their aggregates (Figure 2), is of $6.0 \times 10^{-7}$ einsteins/s. The photonic flux of $3.3 \times 10^{-6}$ einsteins/s in the 295 to 710 nm range is 5.5 times higher. Considering an ideal situation in which 100% of the incident photons furnished by HP, mercury lamps are able to trigger the photocatalytic process, the use of these composites is very advantageous, since these materials pick up 450% more photons than pure $TiO_2$. This

makes these composites very attractive for use in processes induced by solar radiation, the main advantage inherent to these composites, considering that more than 90% of the the incident radiation on biosphere has wavelength above 390 nm. Hence an increase in the population of excited ZnPc aggregates should imply in an electron/hole ratio higher than unity as observed for pure $TiO_2$ [22, 50, 70], besides the other processes triggered by ZnPc excitons.

Additional experiments using a metal vapor lamp to excite the composites exclusively with visible radiation were done and confirmed the effective participation of the visible radiation components in the photocatalytic process (not shown).

The increase in the $\Phi_{HO\bullet}$ value indicates the important role of ZnPc aggregates combined with $TiO_2$ on the photocatalytic processes triggered by these composites. On the other hand, the decrease of the photocatalytic efficiency observed for composites containing ZnPc amounts higher than 2.5% m/m can be attributed to an excessive ZnPc aggregation, which increases the chances of exciton-exciton annihilation affecting the charge transport.

One of the causes for the higher efficiency presented by some of these composites, mainly the one containing 2.5% m/m of ZnPc, can be attributed to the regular distribution and coating thickness of ZnPc on the $TiO_2$ surface. Control of the coating thickness of the photosensitizing dye can prevent/minimize the exciton-exciton annihilation, favoring electron injection in the semiconductor oxide [22, 50, 59, 70] as well as other processes directly mediated by ZnPc excitons. Besides, good electronic coupling between this one and $TiO_2$ is fundamental for the electron transfer process from the exciton [22]. Terasaki et al. [60] using femtosecond spectroscopy technique showed the excited-state dynamics of vanadyl phthalocyanines in various molecular arrangements to be strongly dependent on the molecular arrangements between the formed phases. The composites containing 2.5% m/m of ZnPc, who presented the best photocatalytic performance, possesses the most homogeneous coatings with an average thickness between 5 and 10 nm.

At this point, the available informations are not yet sufficient to propose a detailed mechanism involved in the enhancement of the photocatalytic activity of these composites. However, previous studies give important evidences. Based on the experimental facts reported here and the contribution of other researchers, it is reasonable to assume that the reactions triggered by these composites are based on the formation of electron/hole pairs from $TiO_2$ and also from $ZnPc_{agg}$. For these composites, the key steps which lead to the formation of active species at the solid/solution interface are (a) formation of $e^-/h^+$ pairs by the direct excitation of $TiO_2$ ($\lambda_{exc} \leq 390$ nm); (b) formation of $e^-/ ZnPc^+_{agg}$ by the photoexcitation of $ZnPc_{agg}$; (c) electron transfer from ZnPc excitons to the $TiO_2$ conduction band; (d) charge transport by $ZnPc^+_{agg}$ and its implications, and other reactions triggered by $e^-/ ZnPc^+_{agg}$ pairs.

Ways to prevent/minimize the vulnerability of ZnPc during the photocatalytic process are under study, even though the results presented in this work show that, despite ZnPc degradation, these composites are able to perform efficiently wastewater treatment using solar radiation.

## ACKNOWLEDGMENTS

The authors thank the CNPq, FAPEMIG, CAPES (Brazilian agencies), and the International Bureau of the German Ministry of Education and Research for funding the project WATER BRA 00/015. They also thank Lamark de Oliveira, Edward Thomas Fleury Mendonça Duarte, Eduardo de Faria Franca, Lucas Ferreira de Paula, and Jacques Antonio de Miranda for technical assistance. A. E. H. Machado is particularly indebted to Professor Julien F. C. Boodts for the revision of the English language and valuable suggestions.

## REFERENCES

[1] O. Legrini, E. Oliveros, and A. M. Braun, "Photochemical processes for water treatment," *Chemical Reviews*, vol. 93, no. 2, pp. 671–698, 1993.

[2] G. Palmisano, V. Augugliaro, M. Pagliaro, and L. Palmisano, "Photocatalysis: a promising route for 21st century organic chemistry," *Chemical Communications*, no. 33, pp. 3425–3437, 2007.

[3] M. R. Hoffmann, S. T. Martin, W. Choi, and D. W. Bahnemann, "Environmental applications of semiconductor photocatalysis," *Chemical Reviews*, vol. 95, no. 1, pp. 69–96, 1995.

[4] E. Oliveros, O. Legrini, M. Hohl, T. Müller, and A. M. Braun, "Large scale development of a light-enhanced fenton reaction by optimal experimental design," *Water Science and Technology*, vol. 35, no. 4, pp. 223–230, 1997.

[5] R. L. Ziolli and W. F. Jardim, "Mecanismo de fotodegradação de compostos orgânicos catalisada por $TiO_2$," *Química Nova*, vol. 21, no. 3, pp. 319–325, 1998.

[6] D. M. Blake, "Bibliography of work on photocatalytic removal of hazardous compounds from water and air," Tech. Rep. NREL/TP-430-22197, National Renewable Energy Laboratory, Golden, Colo, USA, 1999.

[7] R. Andreozzi, V. Caprio, A. Insola, and R. Marotta, "Advanced oxidation processes (AOP) for water purification and recovery," *Catalysis Today*, vol. 53, no. 1, pp. 51–59, 1999.

[8] A. E. H. Machado, J. A. de Miranda, R. F. de Freitas, et al., "Destruction of the organic matter present in effluent from a cellulose and paper industry using photocatalysis," *Journal of Photochemistry and Photobiology A*, vol. 155, no. 1–3, pp. 231–241, 2003.

[9] C. Sattler, L. de Oliveira, M. Tzschirner, and A. E. H. Machado, "Solar photocatalytic water detoxification of paper mill effluents," *Energy*, vol. 29, no. 5-6, pp. 835–843, 2004.

[10] C. Sattler, K.-H. Funken, L. de Oliveira, M. Tzschirner, and A. E. H. Machado, "Paper mill wastewater detoxification by solar photocatalysis," *Water Science and Technology*, vol. 49, no. 4, pp. 189–193, 2004.

[11] A. E. H. Machado, T. P. Xavier, D. R. de Souza, et al., "Solar photo-fenton treatment of chip board production waste water," *Solar Energy*, vol. 77, no. 5, pp. 583–589, 2004.

[12] E. T. F. M. Duarte, T. P. Xavier, D. R. de Souza, et al., "Construção e estudos de perfomance de um reator fotoquímico tipo CPC ("Compound Parabolic Concentrator")," *Química Nova*, vol. 28, no. 5, pp. 921–926, 2005.

[13] A. E. H. Machado, J. A. Miranda, C. Sattler, and L. Oliveira, "Compósitos de ftalocianina de zinco e óxido de titânio,

para emprego em processos fotocatalíticos e método para sua obtenção," Brazilian patent no. PI 03009203-3, 2005.

[14] A. E. H. Machado, J. A. Miranda, C. Sattler, and L. Oliveira, "Zinc phthalocyanine and titanium oxide composites used as, e.g. catalyst for wastewater decontamination, prepared by combining titanium oxide and photosensitizer dye capable of potentializing photocatalytical action of titanium oxide," European patent no. EP1646443-A2, 2006.

[15] A. E. H. Machado and V. Velani, "Fotocatalisadores à base de óxido de titânio, dopados com íons de metais de transição, seu processo de preparação e sua aplicação em processos de descontaminação ambiental," Brazilian patent application no. PI 0701120-2, 2007.

[16] V. Iliev, D. Tomova, L. Bilyarska, L. Prahov, and L. Petrov, "Phthalocyanine modified $TiO_2$ or $WO_3$-catalysts for photooxidation of sulfide and thiosulfate ions upon irradiation with visible light," *Journal of Photochemistry and Photobiology A*, vol. 159, no. 3, pp. 281–287, 2003.

[17] G. Mele, R. Del Sole, G. Vasapollo, E. García-López, L. Palmisano, and M. Schiavello, "Photocatalytic degradation of 4-nitrophenol in aqueous suspension by using polycrystalline $TiO_2$ impregnated with functionalized Cu(II)-porphyrin or Cu(II)-phthalocyanine," *Journal of Catalysis*, vol. 217, no. 2, pp. 334–342, 2003.

[18] M. Bellardita, M. Addamo, A. Di Paola, and L. Palmisano, "Photocatalytic behaviour of metal-loaded $TiO_2$ aqueous dispersions and films," *Chemical Physics*, vol. 339, no. 1–3, pp. 94–103, 2007.

[19] C. Sattler, L. Oliveira, and C. Jung, "Volume-doped titanium dioxide composite, useful in photocatalytic procedures for decontaminating wastewater and for removing smells from environment, preferably heterogeneous photo catalysis form, comprises zinc phthalocyanine," German patent no. DE102004053823-A1, 2006.

[20] C. H. Langord, M. K. S. Mak, and A. M. Croch, "Photo-catalyst for refractory waste degradation esp. of PCB residues—comprises wide band semiconductor esp. titanium dioxide, coated with pyridine-contg. polymer and metal porphyrin or phthalocyanine dye," Canadian and US patent no. US4806514-A; CA1287829-C, 1991.

[21] M. Grätzel, "Photoelectrochemical cells," *Nature*, vol. 414, no. 6861, pp. 338–344, 2001.

[22] D. Ino, K. Watanabe, N. Takagi, and Y. Matsumoto, "Electron transfer dynamics from organic adsorbate to a semiconductor surface: zinc phthalocyanine on $TiO_2(110)$," *Journal of Physical Chemistry B*, vol. 109, no. 38, pp. 18018–18024, 2005.

[23] J. M. Rehm, G. L. McLendon, Y. Nagasawa, K. Yoshihara, J. Moser, and M. Grätzel, "Femtosecond electron-transfer dynamics at a sensitizing dye-semiconductor ($TiO_2$) interface," *Journal of Physical Chemistry*, vol. 100, no. 23, pp. 9577–9578, 1996.

[24] M. K. Nazeeruddin, A. Kay, I. Rodicio, et al., "Conversion of light to electricity by *cis*-$X_2$bis(2, 2′-bipyridyl-4, 4′-dicarboxylate)ruthenium(II) charge-transfer sensitizers (X = $Cl^-$, $Br^-$, $I^-$, $CN^-$, and $SCN^-$) on nanocrystalline $TiO_2$ electrodes," *Journal of the American Chemical Society*, vol. 115, no. 14, pp. 6382–6390, 1993.

[25] J. B. Asbury, E. Hao, Y. Wang, H. N. Ghosh, and T. Lian, "Ultrafast electron transfer dynamics from molecular adsorbates to semiconductor nanocrystalline thin films," *Journal of Physical Chemistry B*, vol. 105, no. 20, pp. 4545–4557, 2001.

[26] J. Krüger, R. Plass, L. Cevey, M. Piccirelli, M. Grätzel, and U. Bach, "High efficiency solid-state photovoltaic device due to inhibition of interface charge recombination," *Applied Physics Letters*, vol. 79, no. 13, pp. 2085–2087, 2001.

[27] R. Argazzi, C. A. Bignozzi, G. M. Hasselmann, and G. J. Meyer, "Efficient light-to-electrical energy conversion with dithiocarbamate-ruthenium polypyridyl sensitizers," *Inorganic Chemistry*, vol. 37, no. 18, pp. 4533–4537, 1998.

[28] A. P. Xagas, M. C. Bernard, A. Hugot-Le Goff, N. Spyrellis, Z. Loizos, and P. Falaras, "Surface modification and photosensitisation of $TiO_2$ nanocrystalline films with ascorbic acid," *Journal of Photochemistry and Photobiology A*, vol. 132, no. 1-2, pp. 115–120, 2000.

[29] K. Tennakone, A. R. Kumarasinghe, G. R. R. A. Kumara, K. G. U. Wijayantha, and P. M. Sirimanne, "Nanoporous $TiO_2$ photoanode sensitized with the flower pigment cyanidin," *Journal of Photochemistry and Photobiology A*, vol. 108, no. 2-3, pp. 193–195, 1997.

[30] G. D. Sharma, S. C. Mathur, and D. C. Dube, "Organic photovoltaic solar cells based on some pure and sensitized dyes," *Journal of Materials Science*, vol. 26, no. 24, pp. 6547–6552, 1991.

[31] Y. Hao, M. Yang, C. Yu, et al., "Photoelectrochemical studies on acid-doped polyaniline as sensitizer for $TiO_2$ nanoporous film," *Solar Energy Materials and Solar Cells*, vol. 56, no. 1, pp. 75–84, 1998.

[32] C. Chen, X. Qi, and B. Zhou, "Photosensitization of colloidal $TiO_2$ with a cyanine dye," *Journal of Photochemistry and Photobiology A*, vol. 109, no. 2, pp. 155–158, 1997.

[33] T. Wu, S.-J. Xu, J.-Q. Shen, S. Chen, M.-H. Zhang, and T. Shen, "Photosensitization of $TiO_2$ colloid by hypocrellin B in ethanol," *Journal of Photochemistry and Photobiology A*, vol. 137, no. 2-3, pp. 191–196, 2000.

[34] A. M. Braun, M.-T. Maurette, and E. Oliveros, *Technologie Photochimique*, Presse Romandes, Lausanne, Switzerland, 1986.

[35] R. Gao, J. Stark, D. W. Bahnemann, and J. Rabani, "Quantum yields of hydroxyl radicals in illuminated $TiO_2$ nanocrystallite layers," *Journal of Photochemistry and Photobiology A*, vol. 148, no. 1–3, pp. 387–391, 2002.

[36] T. Nash, "The colorimetric estimation of formaldehyde by means of the Hantzsch reaction," *The Biochemical Journal*, vol. 55, no. 3, pp. 416–421, 1953.

[37] L. Sun and J. R. Bolton, "Determination of the quantum yield for the photochemical generation of hydroxyl radicals in $TiO_2$ suspensions," *Journal of Physical Chemistry*, vol. 100, no. 10, pp. 4127–4134, 1996.

[38] J. Blanco, S. Malato, P. Fernández, et al., "Compound parabolic concentrator technology development to commercial solar detoxification applications," *Solar Energy*, vol. 67, no. 4–6, pp. 317–330, 1999.

[39] K.-H. Funken, C. Sattler, B. Milow, et al., "A comparison of prototype compound parabolic collector-reactors (CPC) on the road to SOLARDETOX technology," *Water Science and Technology*, vol. 44, no. 5, pp. 271–278, 2001.

[40] A. M. Jirka and M. J. Carter, "Micro semi-automated analysis of surface and wastewaters for chemical oxygen demand," *Analytical Chemistry*, vol. 47, no. 8, pp. 1397–1402, 1975.

[41] USEPA, "COD ranges 3–150 mg/L and 20–1500 mg/L COD are USEPA approved (5220 D) for wastewater analyses," *Federal Register*, vol. 45, no. 78, pp. 26811–26812, 1980.

[42] C. C. Leznoff and A. B. P. Lever, Eds., *Phthalocyanines: Properties and Applications*, vol. 1, VCH Publishers, New York, NY, USA, 1990.

[43] C. C. Leznoff and A. B. P. Lever, Eds., *Phthalocyanines: Properties and Applications*, vol. 4, VCH Publishers, New York, NY, USA, 1996.

[44] J. A. de Miranda, A. E. H. Machado, and C. A. de Oliveira, "Comparison of the photodynamic action of methylene blue and zinc phthalocyanine on TG-180 tumoral cells," *Journal of Porphyrins and Phthalocyanines*, vol. 6, no. 1, pp. 43–49, 2002.

[45] G. Ricciardi, A. Rosa, and E. J. Baerends, "Ground and excited states of zinc phthalocyanine studied by density functional methods," *Journal of Physical Chemistry A*, vol. 105, no. 21, pp. 5242–5254, 2001.

[46] K. Szaciłowski, W. Macyk, and G. Stochel, "Synthesis, structure and photoelectrochemical properties of the $TiO_2$-Prussian blue nanocomposite," *Journal of Materials Chemistry*, vol. 16, no. 47, pp. 4603–4611, 2006.

[47] S. Senthilarasu, S. Velumani, R. Sathyamoorthy, et al., "Characterization of zinc phthalocyanine (ZnPc) for photovoltaic applications," *Applied Physics A*, vol. 77, no. 3-4, pp. 383–389, 2003.

[48] D. Meissner and J. Rostalski, "Photovoltaics of interconnected networks," *Synthetic Metals*, vol. 121, no. 1–3, pp. 1551–1552, 2001.

[49] J. Mi, L. Guo, Y. Liu, W. Liu, G. You, and S. Qian, "Excited-state dynamics of magnesium phthalocyanine thin film," *Physics Letters A*, vol. 310, no. 5-6, pp. 486–492, 2003.

[50] M. Hoffmann, "Frenkel and charge-transfer excitons in quasi-one-dimensional molecular crystals with strong intermolecular overlap," Ph.D. thesis, Technischen Universität Dresden, Dresden, Germany, 2000.

[51] J. Mizuguchi and S. Matsumoto, "Molecular distortion and exciton coupling effects in $\beta$ metal-free phthalocyanine," *Journal of Physical Chemistry A*, vol. 103, no. 5, pp. 614–616, 1999.

[52] A. S. Davydov, *Theory of Molecular Excitons*, McGraw-Hill, New York, NY, USA, 1962.

[53] H. Fidder, J. Knoester, and D. A. Wiersma, "Optical properties of disordered molecular aggregates: a numerical study," *Journal of Chemical Physics*, vol. 95, no. 11, pp. 7880–7890, 1991.

[54] O.-K. Kim, J. Je, G. Jernigan, L. Buckley, and D. Whitten, "Super-helix formation induced by cyanine J-aggregates onto random-coil carboxymethyl amylose as template," *Journal of the American Chemical Society*, vol. 128, no. 2, pp. 510–516, 2006.

[55] G. D. Sharma, R. Kumar, and M. S. Roy, "Investigation of charge transport, photo generated electron transfer and photovoltaic response of iron phthalocyanine (FePc): $TiO_2$ thin films," *Solar Energy Materials and Solar Cells*, vol. 90, no. 1, pp. 32–45, 2006.

[56] M. Hilgendorff and V. Sundström, "Ultrafast electron injection and recombination dynamics of dye sensitised $TiO_2$ particles," *Chemical Physics Letters*, vol. 287, no. 5-6, pp. 709–713, 1998.

[57] J. B. Asbury, R. J. Ellingson, H. N. Ghosh, S. Ferrere, A. J. Nozik, and T. Lian, "Femtosecond IR study of excited-state relaxation and electron-injection dynamics of $Ru(dcbpy)_2(NCS)_2$ in solution and on nanocrystalline $TiO_2$ and $Al_2O_3$ thin films," *Journal of Physical Chemistry B*, vol. 103, no. 16, pp. 3110–3119, 1999.

[58] S. Iwai, S. Murata, R. Katoh, M. Tachiya, K. Kikuchi, and Y. Takahashi, "Ultrafast charge separation and exciplex formation induced by strong interaction between electron donor and acceptor at short distances," *Journal of Chemical Physics*, vol. 112, no. 16, pp. 7111–7117, 2000.

[59] V. Gulbinas, M. Chachisvilis, L. Valkunas, and V. Sundström, "Excited state dynamics of phthalocyanine films," *Journal of Physical Chemistry*, vol. 100, no. 6, pp. 2213–2219, 1996.

[60] A. Terasaki, M. Hosoda, T. Wada, et al., "Femtosecond spectroscopy of vanadyl phthalocyanines in various molecular arrangements," *Journal of Physical Chemistry*, vol. 96, no. 25, pp. 10534–10542, 1992.

[61] Y. Sakakibara, R. N. Bera, T. Mizutani, K. Ishida, M. Tokumoto, and T. Tani, "Photoluminescence properties of magnesium, chloroaluminum, bromoaluminum, and metal-free phthalocyanine solid films," *Journal of Physical Chemistry B*, vol. 105, no. 8, pp. 1547–1553, 2001.

[62] G. V. Buxton, C. L. Greenstock, W. P. Helman, and A. B. Ross, "Critical review of rate constants for reactions of hydrated electrons, hydrogen atoms and hydroxyl radicals in aqueous solution," *Journal of Physical and Chemical Reference Data*, vol. 17, no. 2, pp. 513–886, 1988.

[63] N. Motohashi and Y. Saito, "Competitive measurement of rate constants for hydroxyl radical reactions using radiolytic hydroxylation of benzoate," *Chemical and Pharmaceutical Bulletin*, vol. 41, no. 10, pp. 1842–1845, 1993.

[64] C.-Y. Wang, J. Rabani, D. W. Bahnemann, and J. K. Dohrmann, "Photonic efficiency and quantum yield of formaldehyde formation from methanol in the presence of various $TiO_2$ photocatalysts," *Journal of Photochemistry and Photobiology A*, vol. 148, no. 1–3, pp. 169–176, 2002.

[65] N. Serpone, G. Sauvé, R. Koch, et al., "Standardization protocol of process efficiencies and activation parameters in heterogeneous photocatalysis: relative photonic efficiencies $\zeta_r$," *Journal of Photochemistry and Photobiology A*, vol. 94, no. 2-3, pp. 191–203, 1996.

[66] C. Kormann, D. W. Bahnemann, and M. R. Hoffmann, "Photolysis of chloroform and other organic molecules in aqueous $TiO_2$ suspensions," *Environmental Science and Technology*, vol. 25, no. 3, pp. 494–500, 1991.

[67] J. R. Darwent, P. Douglas, A. Harriman, G. Porter, and M. C. Richoux, "Metal phthalocyanines and porphyrins as photosensitisers for reduction of water to hydrogen," *Coordination Chemistry Reviews*, vol. 44, no. 1, pp. 83–126, 1982.

[68] J. G. Moser, *Photodynamic Tumor Therapy: 2nd and 3rd Generation Photosensitizers*, Harwood Academic, Amsterdam, The Netherlands, 1998.

[69] X. H. Qiu, G. V. Nazin, and W. Ho, "Mechanisms of reversible conformational transitions in a single molecule," *Physical Review Letters*, vol. 93, no. 19, Article ID 196806, 4, 2004.

[70] H. Donker, A. van Hoek, W. van Schaik, R. B. M. Koehorst, M. M. Yatskou, and T. J. Schaafsma, "Spectroscopy and photophysics of self-organized zinc porphyrin nanolayers. 2. Transport properties of singlet excitation," *Journal of Physical Chemistry B*, vol. 109, no. 36, pp. 17038–17046, 2005.